Title

Impact of resonant magnetic perturbations on nonlinearly driven modes in drift-wave turbulencea)

Journal

Physics of Plasmas, 19(5)

ISSN

1070-664X

Authors

Leconte, M
Diamond, PH

Publication Date

2012-05-01

DOI

10.1063/1.3694675

Impact of resonant magnetic perturbations on nonlinearly driven modes in drift-wave turbulence[a)]

M. Leconte[1,b)] and P. H. Diamond[1,2]
[1]*WCI Center for Fusion Theory, NFRI, Korea*
[2]*CMTFO and CASS, UCSD, California 92093, USA*

(Received 6 December 2011; accepted 25 February 2012; published online 23 March 2012)

In this work, we study the effects of resonant magnetic perturbations (RMPs) on turbulence, flows, and confinement in the framework of resistive drift wave turbulence. We extend the Hasegawa-Wakatani model to include RMP fields. The effect of the RMPs is to induce a linear coupling between the zonal electric field and the zonal density gradient, which drives the system to a state of electron radial force balance for large $\frac{\delta B_r}{B_0}$. Both the vorticity flux (Reynolds stress) and particle flux are modulated. We derive an extended predator prey model which couples zonal potential and density dynamics to the evolution of turbulence intensity. This model has both turbulence drive and RMP amplitude as control parameters and predicts a novel type of transport bifurcation in the presence of RMPs. We find states that are similar to the ZF-dominated state of the standard predator-prey model, but for which the power threshold is now a function of the RMP strength. For small RMP amplitude, the energy of zonal flows decreases and the turbulence energy increases with $\frac{\delta B_r}{B_0}$, corresponding to a damping of zonal flows. © *2012 American Institute of Physics*. [http://dx.doi.org/10.1063/1.3694675]

I. INTRODUCTION

The target regime for next step fusion devices such as ITER is the H-mode regime (see e.g., Ref. 1 and references herein). However, an intermittent MHD global instability known as edge localized mode (ELM), characteristic of the Hmode regime, threatens the plasma facing components due to strong heat load on the materials. It is, therefore, crucial to control ELMs in future devices and particularly ITER. One possible way of achieving this goal is by applying resonant magnetic perturbations (RMPs), induced by a set of external coils. Experiments on several fusion devices showed a stabilization—i.e., mitigation in some devices and complete suppression in others—of ELMs.[2–8] The precise mechanism responsible for this stabilization is yet not totally understood. As most theories of RMP effects are based on neoclassical physics, see e.g., Ref. 9 and reference herein, the RMP effect on turbulence is, to our knowledge, not broadly considered. There are some turbulence simulations showing a modification of drift-Alfven turbulence by RMPs in the scrape-off layer[10] and the study of effects on relaxation oscillations of transport barriers.[11,12] We emphasize, though, that *the experiments of* Ref. 13 *clearly show* that RMPs have a strong effect on turbulence. We showed, in previous work, that drift-wave turbulence level and associated zonal flows are strongly modified by RMPs, by exploiting a minimal model, namely a generalization of the Hasegawa-Wakatani model.[14] In the present work, we clarify the derivation of the model, and we give more discussion of the basic physics mechanisms of the RMP-drift wave interaction. This article is organized as follows: In Sec. II, we derive the extended Hasegawa-Wakatani model. In Sec. III, we apply a modulational stability analysis using the wave kinetic formalism, to obtain a set of linearly coupled equations for the evolution of a secondary instability, i.e., a zonal mode. We subsequently use the wave kinetic formalism to derive an evolution equation for the turbulence energy, which nonlinearly couples to the zonal mode equations. In Sec. IV, we discuss the different states of the coupled drift waves—zonal mode model and then present some conclusions in Sec. V. The concept of zonal modes is ubiquitous in plasma turbulence, although the term "modes" is seldom used to refer to this concept. For the purpose of illustration, a schematic representation of zonal modes is given [Fig. 1].

II. EXTENDED HASEGAWA-WAKATANI MODEL

In this section, we will derive an **extended** Hasegawa-Wakatani model, describing drift-wave turbulence in presence of RMPs. We start by considering the continuity and vorticity equations for density n and electric potential ϕ

$$\frac{\partial}{\partial t} n + \{\phi, n\} = \nabla_\parallel j_\parallel, \tag{1}$$

$$\rho_s^2 \frac{\partial}{\partial t} \nabla_\perp^2 \phi + \rho_s^2 \{\phi, \nabla_\perp^2 \phi\} = \nabla_\parallel j_\parallel, \tag{2}$$

where the parallel current is

$$j_\parallel = j_{\parallel 0} + \delta j_\parallel. \tag{3}$$

Here, $j_{\parallel 0}$ denotes the unperturbed parallel current, given by

$$j_{\parallel 0} = -D_\parallel \nabla_{\parallel 0} (\phi - n) \tag{4}$$

with $\nabla_{\parallel 0} = \frac{\mathbf{B}}{B} \cdot \nabla$ the unperturbed parallel gradient and $D_\parallel = v_{th,e}^2 / \nu_{ei}$ the parallel diffusivity, $v_{th,e} = \sqrt{k_B T_e / m_e}$

[a)]Paper CI2 6, Bull. Am. Phys. Soc. **56**, 57 (2011).
[b)]Invited speaker. Electronic mail: mleconte@nfri.re.kr.

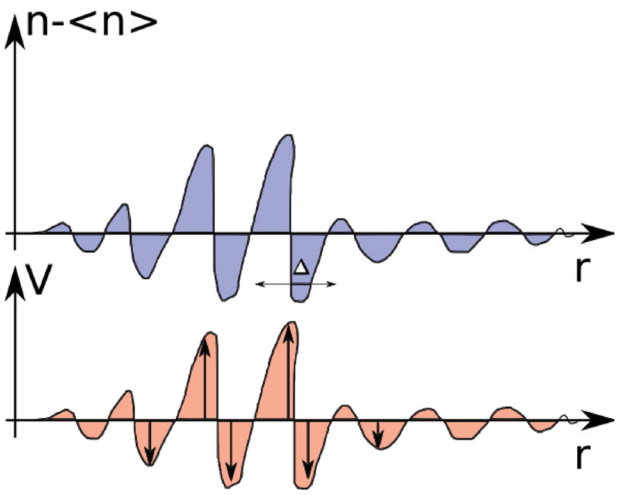

FIG. 1. Illustration of the concept of zonal modes.

being the electron thermal velocity, and ν_{ei} the elecron-ion collisional frequency, which generates a parallel (Spitzer-Harm) resistivity. Here, both the parallel gradient operator $\nabla_\parallel$ and the parallel current perturbation $\delta j_\parallel$ depend on the non-linear parallel gradient perturbation

$$\nabla_\parallel = \nabla_{\parallel 0} + \{\delta\psi^F\}, \tag{5}$$

$$\delta j_\parallel = -D_\parallel\{\delta\psi^F, \phi - n\}, \tag{6}$$

where $\delta\psi^F = \delta\psi^F(x,y,z)$ denotes the magnetic flux perturbation associated to forced-reconnection by RMPs. In the following, we neglect the plasma response and approximate the magnetic flux by its forced value, i.e., we use the approximation: $\delta\psi \sim \delta\psi^F$. Thus, we do not directly address the issue of screening of the external RMP field.

Applying a flux-surface average (the average is performed over unperturbed flux-surfaces, since RMPs only perturb them weakly) to the divergence of the parallel current, yields

$$\langle\nabla_\parallel j_\parallel\rangle = \langle\nabla_{\parallel 0} j_{\parallel 0}\rangle + \langle\{\delta\psi, j_{\parallel 0}\}\rangle + \langle\nabla_{\parallel 0}\delta j_\parallel\rangle + \langle\{\delta\psi, \delta j_\parallel\}\rangle. \tag{7}$$

The first and third terms on the rhs of Eq. (7) vanish when performing the average, and only two terms remain

$$\begin{aligned}\langle\nabla_\parallel j_\parallel\rangle = &-D_\parallel\langle\{\delta\psi, \nabla_{\parallel 0}(\phi - n)\}\rangle \\ &- D_\parallel\langle\{\delta\psi, \{\delta\psi, \phi - n\}\}\rangle,\end{aligned} \tag{8}$$

where we replaced $j_{\parallel 0}$ and $\delta j_\parallel$ by their expression in terms of ϕ, n.

Equation (8) is more clearly written in terms of the radial magnetic field

$$\begin{aligned}\langle\nabla_\parallel j_\parallel\rangle = &-D_\parallel\left\langle\frac{\delta B_x}{B}\frac{\partial}{\partial x}\nabla_{\parallel 0}(\phi - n)\right\rangle \\ &- D_\parallel\left\langle\frac{\delta B_x}{B}\frac{\partial}{\partial x}\left(\frac{\delta B_x}{B}\frac{\partial}{\partial x}(\phi - n)\right)\right\rangle.\end{aligned} \tag{9}$$

Considering disparate-scale interactions, we assume that the scale of the magnetic perturbation, determined by the RMP wavenumber spectrum, is **large** compared to the meso-scale, i.e., the zonal scale

$$\frac{1}{\delta B}\frac{\partial\delta B}{\partial x} \ll \frac{1}{\phi_{ZM}}\frac{\partial\phi_{ZM}}{\partial x}. \tag{10}$$

Hence, the magnetic perturbation is treated as uniform under a zonal average. Using this approximation, the first term on the rhs of expression (9) vanishes upon average and reduces to a single term

$$\langle\nabla_\parallel j_\parallel\rangle = -D_\parallel\left[\frac{\delta B_x}{B}\right]^2\frac{\partial^2}{\partial x^2}(\langle\phi\rangle - \langle n\rangle). \tag{11}$$

We are aware that, by using the disparate-scale approximation, the "resonant" character of the RMP effect is lost, since the resonance with the axisymmetric magnetic field can only occur via the first term on the rhs of Eq. (9), i.e., through the unperturbed parallel gradient $\nabla_{\parallel 0}$. However, we focus in this work on the RMP effect on zonal flow, and this effect is also observed experimentally for non-resonant magnetic field perturbations. We do note though that linear RMP effects on drift-waves or other underlying instabilities depend on resonance, and we will investigate them in a future work.

It is now straightforward to write the flux-surface averaged generalized Hasegawa-Wakatani model

$$\frac{\partial}{\partial t}\langle n\rangle + \frac{\partial}{\partial x}\langle\tilde{v}_x\tilde{n}\rangle = -D_\parallel\left[\frac{\delta B_x}{B}\right]^2\frac{\partial^2}{\partial x^2}(\langle\phi\rangle - \langle n\rangle) \tag{12}$$

$$\begin{aligned}&\rho_s^2\left(\frac{\partial}{\partial t}\langle\nabla_\perp^2\phi\rangle + \mu\langle\nabla_\perp^2\phi\rangle\right) + \rho_s^2\frac{\partial}{\partial x}\langle\tilde{v}_x\nabla_\perp^2\tilde{\phi}\rangle \\ &\quad = -D_\parallel\left[\frac{\delta B_x}{B}\right]^2\frac{\partial^2}{\partial x^2}(\langle\phi\rangle - \langle n\rangle),\end{aligned} \tag{13}$$

where we include a flow damping term μ due to neoclassical ion-ion friction.[16]

Here, $\langle\tilde{v}_x\tilde{n}\rangle, \langle\tilde{v}_x\nabla_\perp^2\tilde{\phi}\rangle$ are, respectively, the (convective) particle flux and the vorticity flux, the latter being linked to the Reynolds stress via the Taylor identity

$$\langle\tilde{v}_x\nabla_\perp^2\tilde{\phi}\rangle = \frac{\partial}{\partial x}\langle\tilde{v}_x\tilde{v}_y\rangle. \tag{14}$$

The physics content of Eqs. (12) and (13) can be understood more easily from the point of view of ambipolarity-breaking responsible for the nonlinear drive of zonal flows. A physical picture of the basic effect of RMPs on zonal modes can be gleaned by considering local ambipolarity-breaking or equivalently, the dynamics of total (normalized) polarization charge Q and total particle number N, in a zonal annulus. The volume-integrated (normalized) vorticity $Q = -\rho_s^2\int\int\int\nabla_\perp^2\phi\, dV$ and volume-integrated density $N = \int\int\int n\, dV$ in a zonal annulus of surface area S_0 and radial width δx evolve according to

$$\frac{dN}{dt} = -S_0\left[\langle \tilde{v}_x \tilde{n}\rangle - \frac{\delta B_x}{B}\langle \delta j_x\rangle\right]_{x-\delta x}^{x+\delta x}, \tag{15}$$

$$\frac{dQ}{dt} = S_0\left[\langle \tilde{v}_x \tilde{\rho}_{\rm pol}\rangle - \frac{\delta B_x}{B}\langle \delta j_x\rangle\right]_{x-\delta x}^{x+\delta x} - \mu Q. \tag{16}$$

Here, the second term on the rhs of both Eqs. (15) and (16) is a radial electron current $\langle j_x\rangle = -\frac{\delta B_x}{B}\frac{\partial}{\partial x}(\langle\phi\rangle - \langle n\rangle)$ that is "weighted" by the RMP amplitude $\frac{\delta B_x}{B}$. Equation (16) shows that the RMP-induced weighted electron current $\frac{\delta B_x}{B}\langle \delta j_x\rangle$ can compete against the (normalized) flux of polarization charge (i.e., normalized vorticity flux) $-\langle \tilde{v}_x \tilde{\rho}_{\rm pol}\rangle = -\rho_s^2\langle \tilde{v}_x \nabla_\perp^2 \tilde{\phi}\rangle$. The last term on the rhs of Eq. (16) represents collisional friction, which damps polarization charge. It is well known that the flux of polarization charge (linked to Reynolds stress) is responsible for the nonlinear generation of zonal flows. In a simple picture, this competition can thus result in a damping of zonal flows. An illustration of this competition between flux of polarization charge and RMP-induced weighted electron current is given [Fig. 2]. However, the actual picture is more complicated, because the RMP-induced weighted electron current also affects the zonal particle balance, via Eq. (15), thus it directly couples the zonal flow dynamics to the turbulent particle flux $\langle \tilde{v}_x \tilde{n}\rangle$. This can be seen by considering an average radial scale Δ for zonal modes, noting that $Q = -\frac{\rho_s^2}{\Delta^2}\int\int\int \phi\, dV$, and combining Eqs. (15) and (16). We then identify a two-fluid polarization charge, i.e., volume-integrated *potential vorticity* $U = Q + N$ and another quantity that we call (volume-integrated) *nonadiabaticity* $H = \int\int\int(\phi - n)dV = -\frac{\Delta^2}{\rho_s^2}Q - N$:

$$\frac{dU}{dt} + \mu Q - S_0[\langle \tilde{v}_x \tilde{\rho}_{\rm pol}\rangle - \langle \tilde{v}_x \tilde{n}\rangle] = 0, \tag{17}$$

$$\frac{dH}{dt} + S_0\left[\langle \tilde{v}_x \tilde{\rho}_{\rm pol}\rangle - \frac{\rho_s^2}{\Delta^2}\langle \tilde{v}_x \tilde{n}\rangle\right] = \frac{1 - \frac{\rho_s^2}{\Delta^2}}{\frac{\rho_s^2}{\Delta^2}} S_0 \frac{\delta B_x}{B}\langle \delta j_x\rangle. \tag{18}$$

Equations (17) and (18) clearly show a complicated coupling between the flux of polarization charge and the particle flux. At marginality, i.e., $d/dt = 0$, Eq. (18) implies that the particle flux is linked to the flux of polarization charge and weighted electron current. Also, Eq. (17) shows that, due to this relation, the polarization charge Q at marginality is set by a balance between the flux of polarization charge, linked to Reynolds stress (source term), the weighted electron current (sink term), and μQ (sink term). The latter effect summarizes our results, namely that zonal flows are damped by the RMP-induced weighted electron current.

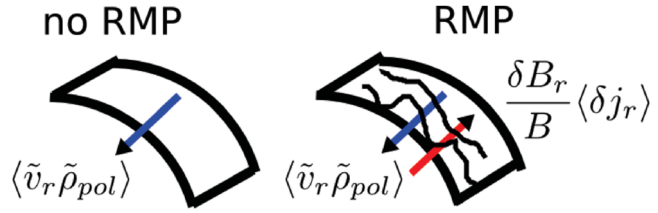

FIG. 2. Competition between flux of polarization charge $\langle \tilde{v}_r \tilde{\rho}_{\rm pol}\rangle$, with $\tilde{\rho}_{\rm pol} = \nabla_\perp^2 \tilde{\phi}$, and RMP-induced weighted radial electron current $\frac{\delta B_r}{B}\langle \delta j_r\rangle$.

We now turn to the modulational analysis. Assuming a slow spatial variation of zonal perturbations of potential (i.e., zonal flows) and density, we introduce modulations (denoted by a "δ") of the particle flux and Reynolds stress

$$\frac{\partial}{\partial t}\delta n = -\frac{\partial}{\partial x}\left(\frac{\delta\langle \tilde{v}_x \tilde{n}\rangle}{\delta n}\delta n + \frac{\delta\langle \tilde{v}_x \tilde{n}\rangle}{\delta \phi}\delta\phi\right) - D_{\rm RMP}\frac{\partial^2}{\partial x^2}(\delta\phi - \delta n), \tag{19}$$

$$\rho_s^2\left(\frac{\partial}{\partial t}\frac{\partial^2}{\partial x^2}\delta\phi + \mu\frac{\partial^2}{\partial x^2}\delta\phi\right) = -\frac{\partial^2}{\partial x^2}\left(\frac{\delta\langle \tilde{v}_x \tilde{v}_y\rangle}{\delta\langle n\rangle}\delta\langle n\rangle + \frac{\delta\langle \tilde{v}_x \tilde{v}_y\rangle}{\delta V}\delta V\right) - D_{\rm RMP}\frac{\partial^2}{\partial x^2}(\delta\phi - \delta n). \tag{20}$$

Applying a Fourier transform with radial wavenumber q, the system can be cast into matrix form

$$\begin{pmatrix} 1 & 0 \\ 0 & \rho_s^2 \end{pmatrix}\frac{d}{dt}\begin{pmatrix} \delta n_q \\ \delta\phi_q \end{pmatrix} = M_q \begin{pmatrix} \delta n_q \\ \delta\phi_q \end{pmatrix}, \tag{21}$$

where the matrix M_q is given by

$$M_q = \begin{pmatrix} -iq\frac{\delta\Gamma_p}{\delta n_q} - D_{\rm turb}q^2 - D_{\rm RMP}q^2 & -iq\frac{\delta\Gamma_p}{\delta\phi_q} + D_{\rm RMP}q^2 \\ -iq\frac{\delta\Pi_{Reyn}}{\delta n_q} + D_{\rm RMP}q^2 & -iq\frac{\delta\Pi_{Reyn}}{\delta\phi_q} - D_{\rm RMP}q^2 \end{pmatrix} \tag{22}$$

with the notation $\Gamma_p = \langle \tilde{v}_x \tilde{n}\rangle, \Pi_{Reyn} = \langle \tilde{v}_x \tilde{v}_y\rangle$. Here, $\frac{\delta\Gamma_p}{\delta n_q}$, etc … refer to modulations.

In Sec. III, we will derive a model for zonal mode growth and subsequently consider the back-reaction of zonal modes on drift-waves. We will then study the coupled drift-wave zonal-mode (DW-ZM) nonlinear system.

III. MODULATIONAL STABILITY ANALYSIS

A. Model for zonal modes

A modulational stability analysis of the system (21), considering the growth of zonal modes in a "bath" of broadband drift-wave turbulence, yields[14]

$$\frac{d}{dt}\delta n_q + q^2\rho_s^2\gamma\epsilon\delta n_q = D_{\rm RMP}q^2(\delta\phi_q - \delta n_q), \tag{23}$$

$$q^2\rho_s^2\left[\frac{d}{dt}\delta\phi_q + \mu\delta\phi_q - \alpha\epsilon(\delta\phi_q - C\delta n_q)\right] = -D_{\rm RMP}q^2(\delta\phi_q - \delta n_q). \quad (24)$$

Here, the model parameters α and γ are the same as in Ref. 15, i.e., without RMPs.

The quantity C can however be evaluated and it is given by

$$C = \sum_{k_\perp\rho_s = k_\perp^{\rm min}\rho_s}^{+\infty} \frac{1}{1+k_\perp^2\rho_s^2} \sim [\tan^{-1}(k_\perp\rho_s)]_1^{+\infty} = \frac{\pi}{4} \simeq 0.8, \quad (25)$$

where we estimated $k_\perp^{\rm min}\rho_s \sim 1$, in accordance with a typical drift-wave spectrum.

B. Back-reaction of zonal modes on drift-waves

In order to close the feedback loop, we now use an equation for the evolution of the drift-wave turbulence energy ϵ. The key concept is *zonal shearing*,[15] i.e., that the turbulence is decorrelated by a radial shear due to the combined zonal $\mathbf{E}\times\mathbf{B}$ flows (linked to zonal potential $\delta\phi_q$) and zonal electron diamagnetic flows (linked to zonal density δn_q). The evolution of turbulence energy—i.e., drift-wave potential enstrophy—is linked to the correlation between turbulence energy and zonal modes, i.e., drift-wave energy changes via the Reynolds stress work on the flow. The shearing effect is responsible for this correlation, which is calculated using the wave kinetic equation (WKE). The details of the derivation are given in Ref. 14. The resulting evolution equation for the turbulence energy is:

$$\frac{d\epsilon}{dt} = \gamma\epsilon - \gamma_{\rm NL}\epsilon^2 - \alpha\epsilon|\delta\phi_q - C\delta n_q|^2. \quad (26)$$

Here, the parameters α, γ have been defined in Subsection III A, and the parameter $\gamma_{\rm NL}$ represents nonlinear damping of drift-waves, i.e., self-saturation. A schematic flowchart of the derivation of the model is given [Fig. 3].

C. Closure of the model

In order to study analytically the dynamics of the coupled DW-zonal mode model given by Eqs. (23) and (24), it is necessary to use a closure relation between zonal density and zonal potential. This follows from the analogy with the linear Hasegawa-Wakatani model where there is only a small deviation from adiabaticity, for $\frac{\gamma_k\omega_k}{D_\parallel k_\parallel^2} \ll 1$, and a large deviation from adiabaticity for $\frac{\gamma_k\omega_k}{D_\parallel k_\parallel^2} >> 1$. To justify this so-called slaving approximation between zonal density and potential and to obtain the form of this relation, we consider two regimes: a weak-RMP regime and a strong-RMP regime. There are two regimes, depending on the evolution timescale of the quantity "$\delta\phi_q - \delta n_q$" as compared to the timescale of the RMP-induced diffusion of zonal modes $\frac{\Delta^2}{D_{\rm RMP}}$ (i.e., $\frac{D_{\rm RMP}}{\Delta^2}$ vs. collisional friction μ), where Δ is an average radial scale of zonal modes

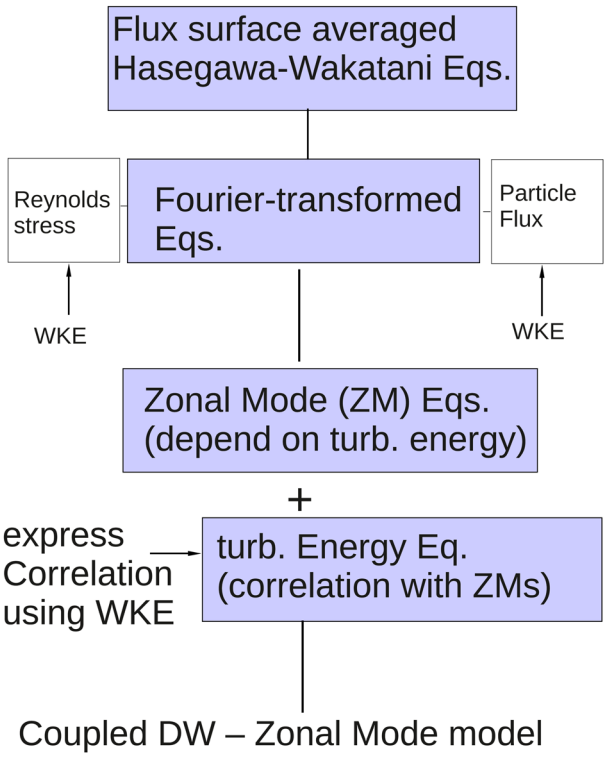

FIG. 3. Flowchart of the derivation for the drift-wave—zonal mode model.

(1) the weak-RMP limit, characterized by a small perturbation of the reference drift wave-zonal flow (DW-ZF) system without RMPs.
(2) the strong-RMP limit, with $\langle E_r\rangle_{\rm ZM} \sim -(k_BT_e/e)\nabla\langle n\rangle_{\rm ZM}$, analogous to weakly non-adiabatic linear drift-waves.

The derivation of a predator-prey model for the weak-RMP regime is straightforward, whereas it is more complicated in the strong-RMP regime, due to the tendency towards zonal electron force balance. To overcome this difficulty, we use in the strong-RMP regime, a simple transformation of the zonal mode equations, equivalent to using "normal variables." The physical interpretation of this transformation, which is also valid for the linear Hasegawa-Wakatani model, is the partial decoupling of the perpendicular dynamics from the parallel dynamics. This partial decoupling is possible because RMPs only affect the parallel dynamics.

1. Weak-RMP regime

In the weak-RMP limit, the RMP-induced diffusion time of zonal modes is long compared to other timescales of the model. We must, therefore, consider the other relevant timescales of the model, namely the turbulent diffusion time $\tau_{\rm turb}(\epsilon)$ and the collisional time $\tau_{\rm coll}$. These characteristic times are given by

$$\tau_{\rm turb}(\epsilon) = \frac{\rho_s^2}{D_{\rm turb}(\epsilon)} = \frac{1}{\gamma\epsilon}, \quad (27)$$

$$\tau_{\rm coll} = \frac{1}{\mu}, \quad (28)$$

$$\tau_{\mathrm{RMP}} = \frac{\Delta^2}{D_{\mathrm{RMP}}}. \tag{29}$$

Here, we considered an average radial scale Δ for zonal modes, i.e., $q^{-1} \sim \Delta$. In the weak-RMP regime, τ_{RMP} is long compared to $\tau_{\mathrm{turb}}(\epsilon)$ and τ_{coll}. There are, therefore, two subregimes: a *turbulence-dominated* regime and a *collision-dominated* regime.

In the turbulence-dominated subregime, turbulent diffusion is the main effect, and the ordering is

$$\tau_{\mathrm{turb}}(\epsilon) \ll \tau_{\mathrm{coll}} \ll \tau_{\mathrm{RMP}}. \tag{30}$$

Since turbulent diffusion only affects zonal density (i.e., zonal electron diamagnetic flows) and not zonal potential (i.e., zonal $E \times B$ flows), the following approximation holds:

$$\tau_{\mathrm{turb}}(\epsilon)\frac{d}{dt}\delta n_q \ll 1. \tag{31}$$

Using approximation Eq. (31), the continuity Eq. (23) yields the following relation between zonal density δn_q, zonal potential $\delta\phi_q$, and turbulence energy ϵ

$$\delta n_q = \frac{D_{\mathrm{RMP}}}{D_{\mathrm{GB}}\epsilon}\delta\phi_q \tag{32}$$

with the *Gyro-Bohm diffusivity* D_{GB} given by

$$D_{\mathrm{GB}} = \rho_s^2\gamma. \tag{33}$$

Here, we only kept contributions to order 1 in $D_{\mathrm{RMP}}/(D_{\mathrm{GB}}\epsilon) \sim (\Delta^2/\rho_s^2)(\tau_{\mathrm{turb}}(\epsilon)/\tau_{\mathrm{RMP}})$. Replacing the zonal density δn_q in Eq. (24) by approximation (32), and dividing by γ, we obtain

$$q^2\rho_s^2\left[\frac{1}{\gamma}\frac{d}{dt}\delta\phi_q + \frac{\mu}{\gamma}\delta\phi_q - \left(\epsilon - C\frac{D_{\mathrm{RMP}}}{D_{\mathrm{GB}}}\right)\frac{\alpha}{\gamma}\delta\phi_q\right] = -\frac{D_{\mathrm{RMP}}q^2}{\gamma}\delta\phi_q. \tag{34}$$

Applying the standard procedure, i.e., multiplying Eq. (34) by the complex-conjugate $\delta\phi_q^*$, multiplying the c.c. of Eq. (56) by $\delta\phi_q$, adding both equations and considering zonal modes having an average radial width Δ, we obtain the following evolution equation for the energy of zonal $\mathbf{E}\times\mathbf{B}$ flows $|V|^2 = |\delta\phi_q|^2$ at scale $q = \Delta^{-1}$, in the weak-RMP regime:

$$\frac{1}{\gamma}\frac{d|V|^2}{dt} + \frac{\mu}{\gamma}|V|^2 - \left(\epsilon - \frac{\Delta^2}{\rho_s^2}\frac{C}{\gamma\tau_{\mathrm{RMP}}}\right)\frac{\alpha}{\gamma}|V|^2 = -\frac{\Delta^2}{\rho_s^2}\frac{|V|^2}{\gamma\tau_{\mathrm{RMP}}}. \tag{35}$$

Here, we considered only contributions at order 1 in $(\gamma\tau_{\mathrm{RMP}})^{-1}$ and replaced D_{GB} by its expression (33). Rearranging terms, the evolution equation for zonal flow energy (35) becomes

$$\frac{1}{\gamma}\frac{d|V|^2}{dt} = \frac{\alpha}{\gamma}\epsilon|V|^2 - \left[\frac{\mu}{\gamma} + \left(C\frac{\alpha}{\gamma} + 1\right)\frac{D_{\mathrm{RMP}}\rho_s^{-2}}{\gamma}\right]|V|^2, \tag{36}$$

where we replaced τ_{RMP} by its expression (29). It can be seen from Eq. (36) that, in the turbulence-dominated subregime, zonal $\mathbf{E}\times\mathbf{B}$ flows are non-linearly generated by primary drift-waves (first term on the rhs), and linearly damped due to collisional flow drag and RMP effects (second term on the rhs). The associated evolution of turbulence energy is given, in the weak-RMP regime, by

$$\frac{d\epsilon}{dt} = \gamma\epsilon - \gamma_{\mathrm{NL}}\epsilon^2 - \alpha\epsilon|V|^2 + 2\frac{D_{\mathrm{RMP}}\rho_s^{-2}}{\gamma}C\alpha|V|^2, \tag{37}$$

where we used $\frac{D_{\mathrm{RMP}}\rho_s^{-2}}{\gamma\epsilon} \ll 1$. Physical insight is difficult to glean directly from Eq. (37), because RMP-coupling term (last term on the rhs) is independent of turbulence energy, and thus cannot be interpreted as a "shearing effect." Rather, we will analyse the saturated states in Subsection IV A.

In the collision-dominated subregime, zonal flow collisional drag takes the principal role, and the ordering is

$$\tau_{\mathrm{coll}} \ll \tau_{\mathrm{turb}}(\epsilon) \ll \tau_{\mathrm{RMP}}. \tag{38}$$

Collisional zonal flow drag only affects zonal $\mathbf{E}\times\mathbf{B}$ flows, since it originates from ion-ion collisions. This implies that the zonal density (i.e., zonal electron diamagnetic flows) is not affected by the zonal flow drag. The zonal potential (i.e., zonal $\mathbf{E}\times\mathbf{B}$ flows) alone will be damped and will thus evolve on a timescale much longer than the collision time τ_{coll} given by expression (28). Hence, the zonal potential dynamics is negligible in this regime, i.e.,

$$\frac{\tau_{\mathrm{coll}}}{\delta\phi_q}\frac{d}{dt}\delta\phi_q \ll 1. \tag{39}$$

Using approximation Eq. (39), Eq. (24) multiplied by τ_{coll} becomes

$$\delta\phi_q - \frac{\alpha}{\gamma}\frac{\tau_{\mathrm{coll}}}{\tau_{\mathrm{turb}}(\epsilon)}(\delta\phi_q - C\delta n_q) = -\frac{\Delta^2}{\rho_s^2}\frac{\tau_{\mathrm{coll}}}{\tau_{\mathrm{RMP}}}(\delta\phi_q - \delta n_q), \tag{40}$$

where we expressed $\alpha\epsilon$ in terms of the turbulent diffusion time $\tau_{\mathrm{turb}}(\epsilon)$. After some algebra, we obtain the following relation (appropriate to the collision-dominated subregime), between zonal potential $\delta\phi_q$, zonal density δn_q, and turbulence ϵ

$$\delta\phi_q = -\left(C\frac{\alpha}{\mu}\epsilon - \frac{\Delta^2}{\rho_s^2}\frac{1}{\mu\tau_{\mathrm{RMP}}}\right)\delta n_q, \tag{41}$$

where we kept only contributions at order 1 in $\tau_{\mathrm{coll}}/\tau_{turb}(\epsilon)$ and replaced the characteristic times by their expression. Replacing the zonal potential $\delta\phi_q$ in Eq. (23) by approximation (41), and dividing by μ, we obtain

$$\frac{1}{\mu}\frac{d}{dt}\delta n_q + \frac{\rho_s^2}{\Delta^2}\frac{\gamma}{\mu}\epsilon\delta n_q = -\frac{\Delta^2}{\rho_s^2}\frac{1}{\mu\tau_{\mathrm{RMP}}}\left[1 + C\frac{\alpha}{\mu}\epsilon\right]\delta n_q, \tag{42}$$

where we considered only contributions at order 1 in $(\mu\tau_{RMP})^{-1}$.

After some algebra, we obtain the evolution of the internal energy $N^2 = |\delta n_q|^2$

$$\frac{1}{\mu}\frac{d|N|^2}{dt} = -\left(\frac{\rho_s^2}{\Delta^2}\frac{\gamma}{\mu} + C\frac{\alpha}{\mu}\frac{D_{\mathrm{RMP}}\rho_s^{-2}}{\mu}\right)\epsilon|N|^2 - \frac{D_{\mathrm{RMP}}\rho_s^{-2}}{\mu}|N|^2. \tag{43}$$

Note that Eq. (43) exhibits no saturated state solutions, it means that zonal electron diamagnetic flows (i.e., zonal density) are both linearly and non-linearly damped to a zero value due turbulent diffusion and RMPs. It follows from the relation (41) that, in the collision-dominated subregime, zonal $\mathbf{E}\times\mathbf{B}$ flows are also damped to a zero value.

2. Strong-RMP regime

We consider the following transformation:

$$\delta u_q = q^2\rho_s^2\delta\phi_q + \delta n_q, \tag{44}$$

$$\delta h_q = \delta\phi_q - \delta n_q. \tag{45}$$

Here, δu_q and δh_q represent, respectively, the *zonal potential vorticity* and the *zonal non-adiabaticity*. Under this transformation, Eqs. (23) and (24) for zonal modes become

$$\frac{d}{dt}\delta u_q + q^2\rho_s^2(C\alpha+\gamma)\epsilon\delta n_q - q^2\rho_s^2(\alpha\epsilon-\mu)\delta\phi_q = 0, \tag{46}$$

$$q^2\rho_s^2\frac{d}{dt}\delta h_q + q^2\rho_s^2(C\alpha - q^2\rho_s^2\gamma)\epsilon\delta n_q - q^2\rho_s^2(\alpha\epsilon-\mu)\delta\phi_q = -(1+q^2\rho_s^2)D_{\mathrm{RMP}}q^2\delta h_q, \tag{47}$$

where the zonal density δn_q and zonal potential $\delta\phi_q$ can themselves be expressed in terms of the new variables, as

$$\delta n_q = \frac{1}{1+q^2\rho_s^2}(\delta u_q - q^2\rho_s^2\delta h_q), \tag{48}$$

$$\delta\phi_q = \frac{1}{1+q^2\rho_s^2}(\delta u_q + \delta h_q). \tag{49}$$

In the strong-RMP limit, the dynamics of zonal nonadiabaticity is slow compared to the RMP-induced diffusion time of zonal modes, i.e., $|\frac{d}{dt}\delta h_q| \ll \frac{D_{\mathrm{RMP}}}{\Delta^2}\delta h_q$. In this regime, the zonal nonadiabaticity dynamics is thus negligible

$$\frac{\tau_{\mathrm{RMP}}}{\delta h_q}\left|\frac{d}{dt}\delta h_q\right| \ll 1 \tag{50}$$

with the RMP-induced diffusion time of zonal modes τ_{RMP} given by expression (29). From Eq. (47), this implies that zonal nonadiabaticity is damped by RMPs, whereas zonal potential vorticity is left unaffected. Simply put, the zonal density dynamics is effectively slaved to zonal potential dynamics. Replacing δn_q and $\delta\phi_q$ by their expressions (48) and (49) in terms of $\delta u_q, \delta h_q$ into Eq. (47), we obtain a relation between zonal nonadiabaticity δh_q, zonal potential vorticity δu_q, and turbulence energy ϵ

$$\frac{q^2\rho_s^2}{1+q^2\rho_s^2}(C\alpha - q^2\rho_s^2\gamma)\epsilon(\delta u_q - q^2\rho_s^2\delta h_q) - \frac{q^2\rho_s^2}{1+q^2\rho_s^2}(\alpha\epsilon-\mu)(\delta u_q + \delta h_q) = -(1+q^2\rho_s^2)D_{\mathrm{RMP}}q^2\delta h_q. \tag{51}$$

After some algebra, we obtain

$$\delta h_q = f_q^{\mathrm{RMP}}(\epsilon)\delta u_q \tag{52}$$

with the function $f_q^{\mathrm{RMP}}(\epsilon)$ given by

$$f_q^{\mathrm{RMP}}(\epsilon) = q^2\rho_s^2\frac{((1-C)\alpha + q^2\rho_s^2\gamma)\epsilon - \mu}{D_{\mathrm{RMP}}q^2}. \tag{53}$$

Here, we used the fact that $q^2\rho_s^2 \ll 1$.

We note parenthetically that the associated relation between zonal density and zonal potential is

$$\delta n_q = [1 - f_q^{\mathrm{RMP}}(\epsilon)]\delta\phi_q. \tag{54}$$

Expression (54) shows that, in addition to the dependence on the linear drive γ, which we obtained by a different approach in Ref. 14, here the relation between zonal density and zonal potential clearly depends also on the collisional drag μ and DW-ZM coupling parameter α.

Now, we may obtain the evolution equation of zonal flow energy, in the strong RMP regime. Rewriting the zonal potential vorticity Eq. (46) in terms of δu_q and δh_q yields

$$(1+q^2\rho_s^2)\frac{d}{dt}\delta u_q = [q^2\rho_s^2(\alpha\epsilon-\mu) - q^2\rho_s^2(C\alpha+\gamma)\epsilon]\delta u_q + [q^2\rho_s^2(\alpha\epsilon-\mu) + q^4\rho_s^4(C\alpha+\gamma)\epsilon]\delta h_q. \tag{55}$$

Note that in the extreme case of very strong RMP amplitude, i.e., for electron force balance $\delta n_q = \delta\phi_q$, zonal adiabaticity is verified $\delta h_q = 0$. In this limit, Eq. (55) states that zonal potential vorticity is nonlinearly generated by DW turbulence (first term in the first bracket on the rhs), but also nonlinearly damped by both turbulent particle diffusion and electron diamagnetic effects (2nd term in the first bracket). Now replacing δh_q by its expression (52), we obtain an evolution equation for zonal potential vorticity, in the strong RMP regime

$$(1+q^2\rho_s^2)\frac{d}{dt}\delta u_q = [q^2\rho_s^2(\alpha\epsilon-\mu) - q^2\rho_s^2(C\alpha+\gamma)\epsilon]\delta u_q + [q^2\rho_s^2(\alpha\epsilon-\mu) + q^4\rho_s^4(C\alpha+\gamma)\epsilon]f_q^{\mathrm{RMP}}(\epsilon)\delta u_q. \tag{56}$$

Applying the standard procedure, i.e., multiplying Eq. (56) by the c.c. δu_q^*, multiplying the c.c. of Eq. (56) by δu_q, adding both equations and considering zonal modes to have an average radial width Δ, i.e., $q \sim \Delta^{-1}$, we obtain the evolution equation for zonal potential enstrophy $|U|^2 = |\delta u_q|^2$ at scale $q = \Delta^{-1}$

$$\frac{d|U|^2}{dt} = \frac{\rho_s^2}{\Delta^2}[(\alpha\epsilon - \mu) - (C\alpha + \gamma)\epsilon]|U|^2 + \frac{\rho_s^2}{\Delta^2}[(\alpha\epsilon - \mu) + \frac{\rho_s^2}{\Delta^2}(C\alpha + \gamma)\epsilon]f_{\mathrm{RMP}}(\epsilon)|U|^2, \quad (57)$$

where we used the fact that $\frac{\rho_s^2}{\Delta^2} \ll 1$.

Here, the function $f_{\mathrm{RMP}}(\epsilon)$ is given by

$$f_{\mathrm{RMP}}(\epsilon) = \frac{\rho_s^2}{\Delta^2}\left[\left((1-C)\alpha\tau_{\mathrm{RMP}} + \frac{\rho_s^2}{\Delta^2}\gamma\tau_{\mathrm{RMP}}\right)\epsilon - \mu\tau_{\mathrm{RMP}}\right]. \quad (58)$$

Note that the quantity $\frac{\tau_{\mathrm{RMP}}}{\tau_{\mathrm{turb}}(\epsilon)}$ is proportional to the ratio between the radial diffusion time of zonal modes due to RMPs and the radial turbulent diffusion time $\tau_{\mathrm{turb}}(\epsilon) = \frac{\rho_s^2}{D_{\mathrm{turb}}(\epsilon)}$, where $D_{\mathrm{turb}}(\epsilon) = \rho_s^2\gamma\epsilon$ is the turbulent diffusivity.

We next derive the associated turbulence energy evolution, in the strong-RMP regime. Expressing δn_q and $\delta\phi_q$ in terms of δu_q and δh_q using relations (48) and (49) and subsequently replacing δh_q by its expression (52), we obtain

$$\frac{d\epsilon}{dt} = \gamma\epsilon - \gamma_{\mathrm{NL}}\epsilon^2 - \left(1 - 2\frac{\rho_s^2}{\Delta^2}\right)\left[(1-C) + \left(1 + \frac{\rho_s^2}{\Delta^2}C\right)f_{\mathrm{RMP}}(\epsilon)\right]^2\alpha\epsilon|U|^2, \quad (59)$$

where we considered an average radial scale for zonal modes, i.e., $q\Delta = 1$, and we used $\rho_s^2/\Delta^2 \ll 1$. Equation (59) suggests that, in the strong-RMP regime, turbulence seems to be more strongly damped by the zonal modes compared to the case without RMPs. This enhanced damping is represented by the contribution proportional to the small function $f_{\mathrm{RMP}}(\epsilon)$ in the last term on the rhs of Eq. (59). It can be understood physically as the increased shearing due to the electron diamagnetic flows. A detailed analysis, which will be given in Sec. IV, is needed to confirm this suggestion.

We summarize our findings, before turning to the analysis of saturated states, and associated power threshold for the transition between different states of the system. Depending on the value of RMP amplitude, there is a weak-RMP regime, with two sub-regimes, depending on the value of collisional friction μ, and a strong-RMP regime.

In the weak-RMP regime $Max\{\frac{D_{\mathrm{RMP}}}{\rho_s^2\mu}, \frac{\alpha D_{\mathrm{RMP}}}{\gamma\rho_s^2\mu}\} \ll 1$, the energy associated with zonal modes, and the corresponding turbulence energy evolve according to

$$\frac{d\epsilon}{dt} = \gamma\epsilon - \gamma_{\mathrm{NL}}\epsilon^2 - \alpha\epsilon|V|^2 + 2\frac{D_{\mathrm{RMP}}\rho_s^{-2}}{\gamma}C\alpha|V|^2, \quad (60)$$

$$\frac{d|V|^2}{dt} = \alpha\epsilon|V|^2 - \left[1 + \left(C\frac{\alpha}{\gamma} + 1\right)\frac{D_{\mathrm{RMP}}\rho_s^{-2}}{\mu}\right]\mu|V|^2. \quad (61)$$

In the strong-RMP regime $\frac{D_{\mathrm{RMP}}}{\rho_s^2\mu} \gg 1$, the potential enstrophy associated to zonal modes and corresponding turbulence energy evolve as

$$\frac{d\epsilon}{dt} = \gamma\epsilon - \gamma_{\mathrm{NL}}\epsilon^2 - \left(1 - 2\frac{\rho_s^2}{\Delta^2}\right)\left[1 - C + \left(1 + \frac{\rho_s^2}{\Delta^2}C\right)f_{\mathrm{RMP}}(\epsilon)\right]^2\alpha\epsilon|U|^2, \quad (62)$$

$$\frac{d|U|^2}{dt} = \frac{\rho_s^2}{\Delta^2}[(\alpha\epsilon - \mu) - (C\alpha + \gamma)\epsilon]|U|^2 + \frac{\rho_s^2}{\Delta^2}[(\alpha\epsilon - \mu) + \frac{\rho_s^2}{\Delta^2}(C\alpha + \gamma)\epsilon]f_{\mathrm{RMP}}(\epsilon)|U|^2 \quad (63)$$

with the small function $f_{\mathrm{RMP}}(\epsilon)$ given by expression (58).

Note that in the case without RMPs corresponding to negligible electron diamagnetic effects, i.e., for $D_{\mathrm{RMP}} = 0$ and $\frac{\delta u_q}{q^2\rho_s^2} = \delta h_q = \delta\phi_q$, Eqs. (60) and (62) become identical, and similarly with Eqs. (61) and (63), recovering the well-known DW-ZF predator-prey model

$$\frac{d\epsilon}{dt} = \gamma\epsilon - \gamma_{\mathrm{NL}}\epsilon^2 - \alpha\epsilon|V|^2. \quad (64)$$

$$\frac{d|V|^2}{dt} = \alpha\epsilon|V|^2 - \mu|V|^2. \quad (65)$$

In Sec. IV, we calculate analytically the energy associated with zonal modes, the corresponding turbulence energy, and we show that RMPs modify the power threshold, or γ threshold, for the transition between possible states.

IV. STATES OF THE COUPLED DRIFT WAVE—ZONAL MODE MODEL

We now study the saturated turbulence states of the system. There are two non-trivial states, i.e., where ϵ and $|V|^2$, ($|U|^2$ in the strong-RMP regime) do not simultaneously vanish. The first possible state is characterized by the absence of zonal modes: $|V|^2 = 0$ ($|U|^2 = 0$ in the strong-RMP regime), and a high turbulence level, while the second possible state is characterized by the presence of zonal modes and a lower turbulence level. To obtain the turbulence energy of the ZM-dominated state, valid for arbitray values of the RMP coupling parameter D_{RMP}, we write the (quasi) linear system (23) and (24) in matrix form with $d/dt = 0$ and set the determinant of the matrix to 0. To obtain the zonal mode energy of the ZM-dominated state, we use a slaving approximation to express the zonal density δn_q in terms of the zonal potential $\delta\phi_q$. The particular form of the slaving approximation $\delta n_q \sim (\gamma\epsilon/D_{\mathrm{RMP}})\delta\phi_q$ used in our previous work[14] is only valid in the weak-RMP regime, whereas in the strong-RMP regime, a different slaving approximation must be used. In the present work, we will use both slaving approixmations, since we wish to study the influence of RMPs on the zonal

mode energy—associated to the L-H transition—in both weak-RMP and strong-RMP regimes.

We first derive the turbulence energy in a saturated state.

A. Saturated turbulence energy states

Writing the (quasi) linear systems (23) and (24) in matrix form with $d/dt = 0$, there are two possible states. The first state, refered to as *Low confinement* state (L) is characterized by no zonal flows, and a high turbulence level, and is unaffected by RMPs

$$\epsilon_L = \frac{\gamma}{\gamma_{\rm NL}}. \tag{66}$$

Here, we obtained ϵ_L by setting $|\delta\phi_q - C\delta n_q|^2 = 0$ in Eq. (26).

The turbulence energy ϵ in the flow-dominated state is obtained by setting the determinant of the (quasi) linear system (23) and (24) to zero. It is given by the following quadratic equation for ϵ:

$$\epsilon^2 - \frac{1}{\alpha}\left[\mu - \frac{D_{\rm RMP}}{\rho_s^2}\left((1-C)\frac{\alpha}{\gamma} - 1\right)\right]\epsilon - \frac{1}{\alpha\gamma}\mu\frac{D_{\rm RMP}}{\rho_s^2} = 0. \tag{67}$$

The physical (positive) solution of Eq. (67) has 2 possible forms, depending on the value of the bracketed term, i.e., on the value of γ, $D_{\rm RMP}$, and μ. At fixed μ, this implies a codimension-2 ($D_{\rm RMP}, \gamma$) bifurcation with RMP parameter $D_{\rm RMP}$ and linear drive, i.e., input power γ. The two subregimes are

1. Low power $\gamma < (1-C)\alpha$

In this case, the quantity $(1-C)\frac{\alpha}{\gamma} - 1$ is positive, and the solution is

$$\epsilon_1 = \frac{1}{2\alpha}\left(\mu - \frac{D_{\rm RMP}}{\rho_s^2}\left|(1-C)\frac{\alpha}{\gamma} - 1\right|\right) + \frac{\sqrt{D_1}}{2} \tag{68}$$

with D_1 the discriminant given by

$$D_1 = \frac{1}{\alpha^2}\left(\mu - \frac{D_{\rm RMP}}{\rho_s^2}\left|(1-C)\frac{\alpha}{\gamma} - 1\right|\right)^2 + \frac{4}{\alpha\gamma}\mu\frac{D_{\rm RMP}}{\rho_s^2}. \tag{69}$$

2. High power $\gamma > (1-C)\alpha$

In this case, the quantity $(1-C)\frac{\alpha}{\gamma} - 1$ is negative, and the solution is

$$\epsilon_2 = \frac{1}{2\alpha}\left(\mu + \frac{D_{\rm RMP}}{\rho_s^2}\left|1 - (1-C)\frac{\alpha}{\gamma}\right|\right) + \frac{\sqrt{D_2}}{2} \tag{70}$$

with D_1 the discriminant given by

$$D_2 = \frac{1}{\alpha^2}\left(\mu + \frac{D_{\rm RMP}}{\rho_s^2}\left|1 - (1-C)\frac{\alpha}{\gamma}\right|\right)^2 + \frac{4}{\alpha\gamma}\mu\frac{D_{\rm RMP}}{\rho_s^2}. \tag{71}$$

In the weak-RMP regime $\frac{D_{\rm RMP}}{\rho_s^2\mu} \ll 1$, we see after some algebra that the turbulence energy is identical in both subregimes

$$\epsilon_1 \sim \epsilon_2 \sim \left[1 + \left(C\frac{\alpha}{\gamma} + 1\right)\frac{D_{\rm RMP}}{\rho_s^2\mu}\right]\frac{\mu}{\alpha}. \tag{72}$$

In the strong-RMP regime $\frac{D_{\rm RMP}}{\rho_s^2\mu} \gg 1$, we see after some algebra that the turbulence energies of the two subregimes are different

$$\epsilon_1 \sim \left[1 + \left(\frac{\alpha}{(1-C)\alpha - \gamma} - 1\right)\frac{\rho_s^2\gamma\mu}{[(1-C)\alpha - \gamma]D_{\rm RMP}}\right] \times \left[(1-C)\frac{\alpha}{\gamma} - 1\right]\frac{D_{\rm RMP}}{\rho_s^2\alpha} \tag{73}$$

$$\epsilon_2 \sim \left[1 + \left(\frac{\alpha}{\gamma - (1-C)\alpha} + 1\right)\frac{\rho_s^2\gamma\mu}{[\gamma - (1-C)\alpha]D_{\rm RMP}}\right] \times \left[1 - (1-C)\frac{\alpha}{\gamma}\right]\frac{D_{\rm RMP}}{\rho_s^2\alpha}. \tag{74}$$

We now separate our analysis into the weak-RMP and strong-RMP regimes, to calculate the zonal mode energy.

B. Weak-RMP regime

The turbulence energy (72) can be written

$$\epsilon = [1 + g(\gamma)\hat{D}_{\rm RMP}]\frac{\mu}{\alpha}. \tag{75}$$

This includes a normalized RMP parameter $\hat{D}_{\rm RMP}$, and a coefficient $g(\gamma)$, depending on linear drive γ, given, respectively, by

$$\hat{D}_{\rm RMP} = \frac{D_{\rm RMP}}{\rho_s^2\mu}. \tag{76}$$

$$g(\gamma) = C\frac{\alpha}{\gamma} + 1. \tag{77}$$

Expression (75) is identical to the expression we obtained in our previous work in the weak-RMP limit.[14]

Next, using Eq. (60) in a saturated state, we express, in the weak-RMP regime, the zonal flow energy $|V|^2$ in terms of the turbulence energy

$$|V|^2 = \left(1 + 2\frac{D_{\rm RMP}}{\rho_s^2\gamma\epsilon}C\right)\left(\frac{\gamma}{\alpha} - \frac{\gamma_{\rm NL}}{\alpha}\epsilon\right), \tag{78}$$

where we used $D_{\rm RMP}/(\rho_s^2\gamma\epsilon) \ll 1$.

Replacing ϵ by its expression (75), we obtain the zonal flow energy in the weak-RMP regime

$$|V|^2 = \left(1 + (1 - g(\gamma))2\hat{D}_{\rm RMP}\frac{\alpha}{\gamma}C\right) \times \left(\frac{\gamma}{\alpha} - [1 + g(\gamma)\hat{D}_{\rm RMP}]\frac{\gamma_{\rm NL}\mu}{\alpha^2}\right). \tag{79}$$

Equation (79) shows that the threshold $\gamma = \gamma_c^{\text{weak}}$ (linked to the power threshold at transition $P = P_c$) for the transition from the low confinement regime (L) to the enhanced confinement regime (ZM-dominated) in the weak-RMP regime is given by

$$\gamma - \left[1 + \left(C\frac{\alpha}{\gamma} + 1\right)\hat{D}_{\text{RMP}}\right]\frac{\gamma_{\text{NL}}\mu}{\alpha} = 0, \tag{80}$$

where we replaced $g(\gamma)$ by its expression (77).

Note that in this model, $\gamma = \gamma(\frac{a}{L_n})$ with L_n the mean density gradient scale-length, and the particle flux is $\Gamma = -D\nabla\langle n\rangle$, corresponding to $\gamma = \gamma(\frac{a}{L_n})$ and $Q = -\chi\nabla p$, with p the pressure, χ the collisional diffusivity and Q the energy flux i.e., input power, since we assume uniform temperature. Equation (80) yields a quadratic equation for γ with physical solution (i.e., positive since power is a positive quantity)

$$\gamma_c^{\text{weak}} = \left[1 + \left(1 + C\frac{\alpha^2}{\gamma_{\text{NL}}\mu}\right)\hat{D}_{\text{RMP}}\right]\frac{\gamma_{\text{NL}}\mu}{\alpha}. \tag{81}$$

In presence of RMPs $\hat{D}_{\text{RMP}} > 0$, the power threshold (81) is clearly increased over its reference value without RMPs. The relative threshold variation is given by

$$\frac{\gamma_c^{\text{weak}} - \gamma_c^0}{\gamma_c^0} = \left(1 + C\frac{\alpha^2}{\gamma_{\text{NL}}\mu}\right)\hat{D}_{\text{RMP}}. \tag{82}$$

Hence, our model predicts, in the weak-RMP regime, an increase of the L-H power threshold, near transition. Such an increase in power threshold has been observed experimentally.[6,17]

We now consider the analysis of the strong-RMP regime.

C. Strong-RMP regime

We seek the zonal potential enstrophy $|U|^2$. To obtain it, we use the turbulence energy evolution equation, in a saturated state. The evolution equation for turbulence energy, given by Eq. (26), can be expressed in terms of zonal potential vorticity δu_q and zonal nonadiabaticity δh_q. In terms of δu_q and δh_q, it reads

$$\frac{d\epsilon}{dt} = \gamma\epsilon - \gamma_{\text{NL}}\epsilon^2 - \alpha\epsilon\left|(1-C)\delta u_q + \left(1 - \frac{\rho_s^2}{\Delta^2}C\right)\delta h_q\right|^2, \tag{83}$$

where we used $q\rho_s \sim \rho_s\Delta^{-1} \ll 1$.

Replacing δh_q by its expression (52), we obtain

$$\frac{d\epsilon}{dt} = \gamma\epsilon - \gamma_{\text{NL}}\epsilon^2 - \alpha\epsilon\left[1 - C + \left(1 - \frac{\rho_s^2}{\Delta^2}C\right)f_{\text{RMP}}(\epsilon)\right]^2|U|^2. \tag{84}$$

In steady-state, this yields

$$\gamma - \gamma_{\text{NL}}\epsilon - \alpha\left[1 - C + \left(1 - \frac{\rho_s^2}{\Delta^2}C\right)f_{\text{RMP}}(\epsilon)\right]^2|U|^2 = 0. \tag{85}$$

The potential entrophy of zonal modes, in the strong-RMP regime, is thus given by

$$|U|^2_{1,2} = \frac{1}{(1-C)^2}\left[1 - 2\left(1 - \frac{\rho_s^2}{\Delta^2}C\right)\frac{f_{\text{RMP}}(\epsilon_{1,2})}{1-C}\right]\frac{\gamma - \gamma_{\text{NL}}\epsilon_{1,2}}{\alpha} \tag{86}$$

with $\epsilon_{1,2}$ given by expression (73) and (74), respectively.

Expression (86) clearly shows that, in the strong-RMP regime ($|f_{\text{RMP}}(\epsilon)| \ll 1$), the potential enstrophy associated to zonal modes is a decreasing function of the turbulence energy. The threshold for the transition from low confinement state $\epsilon = \gamma/\gamma_{\text{NL}}, |U|^2 = 0$ to flow-dominated state $\epsilon = \epsilon_{1,2}, |U|^2 = |U|^2_{1,2}$ is given for the first subregime $\gamma < (1-C)\alpha$ by

$$\gamma - \left[1 + \left(\frac{\alpha}{(1-C)\alpha - \gamma} - 1\right)\frac{\rho_s^2\gamma\mu}{[(1-C)\alpha - \gamma]D_{\text{RMP}}}\right] \times \left((1-C)\frac{\alpha}{\gamma} - 1\right)\frac{\gamma_{\text{NL}}D_{\text{RMP}}}{\rho_s^2\alpha} = 0 \tag{87}$$

and for the second subregime $\gamma > (1-C)\alpha$ by

$$\gamma - \left[1 + \left(\frac{\alpha}{\gamma - (1-C)\alpha} + 1\right)\frac{\rho_s^2\gamma\mu}{[\gamma - (1-C)\alpha]D_{\text{RMP}}}\right] \times \left(1 - (1-C)\frac{\alpha}{\gamma}\right)\frac{\gamma_{\text{NL}}D_{\text{RMP}}}{\rho_s^2\alpha} = 0. \tag{88}$$

Note that in the extreme limit $\frac{\rho_s^2\mu}{D_{\text{RMP}}} \to 0$, the second term in the bracketed terms of Eqs. (87) and (88) vanish and the associated power thresholds are

$$\gamma_1^{\text{strong}} \sim (1-C)\alpha, \tag{89}$$

$$\gamma_2^{\text{strong}} \sim \left[1 - (1-C)\frac{\rho_s^2\alpha^2}{\gamma_{\text{NL}}D_{\text{RMP}}}\right]\frac{\gamma_{\text{NL}}D_{\text{RMP}}}{\rho_s^2\alpha}. \tag{90}$$

As opposed to the weak-RMP regime where the power threshold was set mainly by the flow friction μ, in the strong-RMP regime, we see from Eqs. (89) and (90) that the power threshold is set mainly by the DW-zonal mode nonlinear coupling parameter α or by the RMP-induced flow friction $\frac{D_{\text{RMP}}}{\rho_s^2}$, depending on the subregime considered. The latter subregime is similar to the weak-RMP regime, i.e., zonal modes are damped and the power threshold varies approximately linearly with RMP coupling parameter D_{RMP}. In the former subregime however, the power threshold is approximately independent of the RMP coupling parameter, i.e., the RMP effect saturates. This suggests that for this regime of parameters, there exist a critical RMP amplitude above which RMPs have almost no impact on the L-H transition. We will investigate more deeply this regime in the future.

V. CONCLUSION

This work was motivated by recent experimental results showing evidence for the damping of geodesic acoustic mode (GAM) zonal flows by resonant magnetic perturbations, i.e., a damping of the $m = 0$, $n = 0$ potential

component of the GAMs.[13] GAMs are secondary structures which are caused by the coupling between axisymmetric $E \times B$ flows and pressure up-down asymmetry due to the toroidal curvature.[18,19] They have an oscillatory nature, with a frequency ω_{GAM} given by $\omega_{GAM}^2 \sim 2c_s^2/R^2$ with c_s the sound speed and R the major radius. In the present work, to keep analytical calculations tractable, we considered the modulational growth of non-oscillatory $E \times B$ flows (also called zero-frequency zonal flows). Since GAMs are a type of zonal flows,[18] our analysis can partly explain the observations of Ref. 13. However, there is an additional coupling mechanism for GAM, due to toroidal curvature. For the sake of completeness, we give a heuristic model for the damping of GAMs [Appendix]. It seems to show that, in presence of resonant magnetic perturbations, the axisymmetric pressure (here, we consider density) component n_{00}, as well as the up-down asymmetric potential component ϕ_{01} can no longer be neglected and play an important role. RMPs directly couple ϕ_{00} to n_{00}, as in the case of zero-frequency zonal flows (the model developed throughout this article), but also directly couple n_{01} to ϕ_{01}. Note that parallel flows, which are also a component of GAMs, are not taken into account in the heuristic model given in Appendix. We show in Appendix that, in order to fully describe RMP effect on GAMs, one must consider the dynamics of axisymmetric density $\langle n \rangle$ and up-down asymmetric potential $\langle \phi \sin\theta \rangle$, with θ the poloidal angle. Nonetheless, some physical insight can be gleaned from the heuristic model (A7) and (A8). The first term on the rhs of Eq. (A8) shows that the weighted radial current $\frac{\delta B_r}{B}\langle \delta j_x \rangle$ can compete against the flux of polarization charge $\langle \tilde{v}_x \tilde{\rho}_{pol} \rangle$, resulting in an RMP-induced damping of polarization charge Q_0. This is analog to the RMP-induced damping of zero-frequency zonal flows shown throughout this article. A new feature of this heuristic model for GAMs, compared to zero-frequency zonal flows, is the fact that the contribution $\frac{\delta B_r}{B}\langle j_\parallel \sin\theta \rangle$—also a sort of weighted current—can compete against the flux $\langle \tilde{v}_x \tilde{n} \sin\theta \rangle$. Note that the latter flux is a particle flux, but it is different from the "standard" particle flux $\langle \tilde{v}_x \tilde{n} \rangle$ considered throughout this work. According to Ref. 18, the flux $\langle \tilde{v}_x \tilde{n} \sin\theta \rangle$ is the main drive for GAMs. Hence, the competition of the weighted current against this flux gives a possible explanation for the damping of GAMs. We now summarize the main results of this article concerning the zero-frequency zonal flows.

In this work, we first generalized the Hasegawa-Wakatani model to include RMPs, as a tool to analyse the effect of RMPs on zonal flow dynamics. For this purpose, we then applied a modulational stability analysis to our model, using the wave kinetics formalism. Associated to an evolution equation for DW turbulence energy, we obtained a coupled DW-ZM model in two different regimes, depending on the RMP coupling parameter $\hat{D}_{\mathrm{RMP}} = \frac{D_{\mathrm{RMP}}}{\rho_s^2 \mu}$, with the diffusion coefficient $D_{\mathrm{RMP}} = \frac{\delta B_r^2}{B^2} D_\parallel$ representing the RMP-induced diffusion of zonal modes. This model is a generalization of the standard DW-ZF model predator-prey model.[15] The weak-RMP regime, characterized by $\frac{D_{\mathrm{RMP}}}{\rho_s^2 \mu} \ll 1$, exhibits only small modifications compared to the reference case without RMPs. The strong-RMP regime, characterized by $\frac{D_{\mathrm{RMP}}}{\rho_s^2 \mu} \gg 1$, shows a tendency to (mesoscale) electron force balance. The DW-ZM model has two possible states, thus a bifurcation is possible for a critical value of the linear drive, i.e., input power. Below threshold, the system is in a low confinement mode (Lmode-like), characterized by a high turbulence energy and no zonal modes. Above threshold, the system is characterized by an enhanced confinement, i.e., lower turbulence energy and the presence of zonal modes. This is similar to the reference case without RMPs. However, in presence of RMPs, the threshold for the bifurcation between these two states depends on RMP amplitude. In the weak-RMP regime, the relative threshold variation scales linearly with the RMP coupling parameter. Hence, in the weak-RMP regime, the variation in power threshold scales as the square of RMP amplitude $\frac{\delta B_r}{B}$, as the inverse of the collisional zonal flow friction μ, and as the square-inverse of the sound gyroradius ρ_s. We note that stochastization of magnetic field lines not taken into account in our model can play an important role and will be studied elsewhere. Such field-line stochastization effects can be modeled in part, using a concept of hyper-resistivity—increasing with RMP amplitude—in Ohm's law relating $\delta j_\parallel$ to $\delta\phi$ and δn.

ACKNOWLEDGMENTS

The authors would like to thank Y. Xu and G. Mc Kee for usefull discussion. This work was supported by the World Class Institute (WCI) Program of the National Research Foundation of Korea (NRF) funded by the Ministry of Education, Science and Technology of Korea (MEST) (NRF Grant No. WCI 2009-001).

APPENDIX: HEURISTIC MODEL FOR RMP EFFECT ON GAMS

For the sake of completeness, we extend the polarization charge balance model Eqs. (15) and (16) to include toroidal curvature effects. This yields a heuristic model for GAMs. We start from our generalized Hasegawa-Wakatani model (1) and (2), including curvature terms

$$\frac{\partial}{\partial t} n + \{\phi, n\} - \nabla_\parallel j_\parallel = 2\hat{G}\phi, \tag{A1}$$

$$\rho_s^2 \frac{\partial}{\partial t} \nabla_\perp^2 \phi + \rho_s^2 \{\phi, \nabla_\perp^2 \phi\} - \nabla_\parallel j_\parallel = -\hat{G} n, \tag{A2}$$

where the curvature operator $\hat{G}$ is given by $\hat{G} = \sin\theta \frac{\partial}{\partial x} + \frac{cos\theta}{r_0}\frac{\partial}{\partial \theta}$, with r_0 a radius of reference.

Multiplying Eq. (A1) by $\sin\theta$ and flux-surface averaging the resulting equations, we obtain

$$\frac{\partial}{\partial t}\langle n \sin\theta \rangle + \frac{\partial}{\partial x}\langle \tilde{v}_x \tilde{n} \sin\theta \rangle - \langle \sin\theta \nabla_\parallel j_\parallel \rangle = \frac{\partial}{\partial x}\langle \phi \rangle, \tag{A3}$$

$$\rho_s^2 \frac{\partial}{\partial t}\frac{\partial^2}{\partial x^2}\langle \phi \rangle + \rho_s^2 \frac{\partial}{\partial x}\langle \tilde{v}_x \nabla_\perp^2 \tilde{\phi} \rangle - \langle \nabla_\parallel j_\parallel \rangle = -\frac{\partial}{\partial x}\langle n \sin\theta \rangle. \tag{A4}$$

We now define the following quantities:

$$N_0 = \iiint \langle n \rangle dV, \quad Q_0 = -\frac{\rho_s^2}{\Delta^2} \iiint \langle \phi \rangle dV, \tag{A5}$$

and

$$N_1 = \iiint \langle n \sin\theta \rangle dV, \quad Q_1 = -\frac{\rho_s^2}{\Delta^2} \iiint \langle \phi \sin\theta \rangle dV. \tag{A6}$$

Integrating radially Eqs. (A3) and (A4), we obtain the following heuristic model for RMP effect on GAMs:

$$\frac{dN_1}{dt} = -S_0 [\langle \tilde{v}_x \tilde{n} \sin\theta \rangle - \frac{\delta B_x}{B} \langle j_\parallel \sin\theta \rangle]_{x-\delta x}^{x+\delta x} - \frac{1}{r_0} \iiint \frac{\delta B_\theta}{B} \langle j_\parallel \cos\theta \rangle dV + \iiint \frac{\partial}{\partial x} \langle \phi \rangle dV, \tag{A7}$$

$$\frac{dQ_0}{dt} = S_0 \left[\langle \tilde{v}_x \tilde{\rho}_{pol} \rangle - \frac{\delta B_x}{B} \langle \delta j_x \rangle \right]_{x-\delta x}^{x+\delta x} - \mu Q_0 + \iiint \frac{\partial}{\partial x} \langle n \sin\theta \rangle dV. \tag{A8}$$

Here, the standard coupling giving GAMs their oscillatory nature occurs through the last term on the rhs of Eqs. (A7) and (A8).

The RMP-induced weighted radial current $\frac{\delta B_x}{B} \langle \delta j_x \rangle$ present in Eq. (A8) directly couples Q_0 to the evolution of N_0, as in the case for zero-frequency zonal flows

$$\left[\frac{\delta B_x}{B} \langle \delta j_x \rangle \right]_{x-\delta x}^{x+\delta x} \sim -D_\parallel \left[\frac{\delta B_x}{B} \right]^2 \frac{1}{\Delta} \left(\frac{\Delta^2}{\rho_s^2} (-Q_0) - N_0 \right). \tag{A9}$$

Additionally, the RMP-induced contribution $\frac{\delta B_x}{B} \langle j_\parallel \sin\theta \rangle$ in Eq. (A7) directly couples N_1 to the evolution of Q_1

$$\left[\frac{\delta B_x}{B} \langle j_\parallel \sin\theta \rangle \right]_{x-\delta x}^{x+\delta x} \sim -D_\parallel \left[\frac{\delta B_x}{B} \right]^2 \frac{1}{\Delta} \left(\frac{\Delta^2}{\rho_s^2} (-Q_1) - N_1 \right). \tag{A10}$$

Hence, to describe RMP effect on GAM Zonal Flows, one needs to write evolution equations for N_0 and Q_1, in addition to Eqs. (A7) and (A8). As we only give a heuristic model in the present work, we will present the full set somewhere else.

[1]F. Wagner, Plasma Phys. Controlled Fusion **49**, B1 (2007).
[2]T. E. Evans, R. A. Moyer, P. R. Thomas, J. G. Watkins, T. H. Osborne, J. A. Boedo, E. J. Doyle, M. E. Fenstermacher, K. H. Finken, R. J. Groebner, M. Groth, J. H. Harris, R. J. La Haye, C. J. Lasnier, S. Masuzaki, N. Ohyabu, D. G. Pretty, T. L. Rhodes, H. Reimerdes, D. L. Rudakov, M. J. Schaffer, G. Wang, and L. Zeng, Phys. Rev. Lett. **92**, 235003 (2004).
[3]K. H. Burrell, T. E. Evans, E. J. Doyle, M. E. Fenstermacher, R. J. Groebner, A. W. Leonard, R. A. Moyer, T. H. Osborne, M. J. Schaffer, P. B. Snyder, P. R. Thomas, W. P. West, J. A. Boedo, A. M. Garofalo, P. Gohil, G. L. Jackson, R. J. La Haye, C. J. Lasnier, H. Reimerdes, T. L. Rhodes, J. T. Scoville, W. M. Solomon, D. M. Thomas, G. Wang, J. G. Watkins, and L. Zeng, Plasma Phys. Controlled Fusion **47**, B37 (2005).
[4]Y. Liang, H. R. Koslowski, P. R. Thomas, E. Nardon, S. Jachmich, A. Alfier, G. Arnoux, Y. Baranov, M. Becoulet, M. Beurskens, R. Coelho, Th. Eich, E. De La Luna, W. Fundamenski, S. Gerasimov, C. Giroud, M. P. Gryaznevich, D. Harting, A. Huber, A. Kreter, L. Moreira, V. Parail, S. D. Pinches, S. Saarelma, O. Schmitz, and JET-EFDA contributors, Nucl. Fusion **50**, 025013 (2010).
[5]K. H. Finken, B. Unterberg, Y. Xu, S. S. Abdullaev, M. Jakubowski, M. Lehnen, M. F. M. de Bock, S. Bozhenkov, S. Brezinsek, C. Busch, I. G. J. Classen, J. W. Coenen, D. Harting, M. von Hellermann, S. Jachmich, R. J. E. Jaspers, Y. Kikuchi, A. Kramer-Flecken, Y. Liang, M. Mitri, P. Peleman, A. Pospieszczyk, D. Reiser, D. Reiter, U. Samm, D. Schega, O. Schmitz, S. Soldatov, M. Van Schoor, M. Vergote, R. R. Weynants, R. Wolf, O. Zimmermann, and TEXTOR Team, Nucl. Fusion **47**, 522 (2007).
[6]A. Kirk, Y. Liu, E. Nardon, P. Tamain, P. Cahyna, I. Chapman, P. Denner, H. Meyer, S. Mordijck, D. Temple, and MAST Team, Plasma Phys. Controlled Fusion **53**, 065011 (2011).
[7]W. Suttrop, T. Eich, J. C. Fuchs, S. Gunter, A. Janzer, A. Herrmann, A. Kallenbach, P. T. Lang, T. Lunt, M. Maraschek, R. M. McDermott, A. Mlynek, T. Putterich, M. Rott, T. Vierle, E. Wolfrum, Q. Yu, I. Zammuto, H. Zohm, and ASDEX Upgrade Team, Phys. Rev Lett. **106**, 225004 (2011).
[8]Y. M. Jeon, J.-K. Park, S. W. Yoon, J. G. Bak, W. H. Ko, S. G. Lee, K. D. Lee, G. S. Yun, Y. U. Nam, W. C. Kim, J.-G. Kwak, G. S. Lee, H. K. Kim, H. L. Yang, and KSTAR Team, Phys. Rev. Lett., "Suppression of Edge Localized Modes in High-Confinement KSTAR Plasmas by Non-Axisymmetric Magnetic Perturbations" (to be published).
[9]J. D. Callen, Nucl. Fusion **51**, 094026 (2011).
[10]D. Reiser, Phys. Plasmas **14**, 082314 (2007).
[11]M. Leconte, P. Beyer, X. Garbet, and S. Benkadda, Nucl. Fusion **50**, 054008 (2010).
[12]P. Beyer, F. de Solminihac, M. Leconte, X. Garbet, F. L. Waelbroeck, A. I. Smolyakov, and S. Benkadda, Plasma Phys. Controlled Fusion **53**, 054003 (2011).
[13]Y. Xu, D. Carralero, C. Hidalgo, S. Jachmich, P. Manz, E. Martines, B. van Milligen, M. A. Pedrosa, M. Ramisch, I. Shesterikov, C. Silva, M. Spolaore, U. Stroth, and N. Vianello, Nucl. Fusion **51**, 063020 (2011).
[14]M. Leconte and P. H. Diamond, Phys. Plasmas **18**, 082309 (2011).
[15]P. H. Diamond, S.-I. Itoh, K. Itoh, and T. S. Hahm, Plasma Phys. Controlled Fusion **47**, R35 (2005).
[16]A. B. Hassam and R. M. Kulsrud, Phys. Fluids **21**, 2271 (1978).
[17]F. Ryter, R. Fisher, B. Kurzan, T. Putterich, S. K. Rathgeber, W. Suttrop, E. Viezzer, E. Wolfrum, and ASDEX Upgrade Team, in *Proceedings of the 13th International Workshop on H-Mode Physics and Transport Barriers*, Oxford, UK, Oct 10–12, 2011; F. Ryter, S. K. Rathgeber, E. Viezzer, W. Suttrop, A. Burckhart, R. Fischer, B. Kurzan, S. Potzel, T. Putterich, and ASDEX Upgrade Team, "L-H transition in the presence of magnetic perturbations in ASDEX Upgrade," Nucl. Fusion (accepted).
[18]K. Hallatschek and D. Biskamp, Phys. Rev. Lett. **86**, 1223 (2001).
[19]K. Miki and P. H. Diamond, Nucl. Fusion **51**, 103003 (2011).